Bifurcation in Dynamical Systems.
Deterministic Chaos. Quantum Chaos

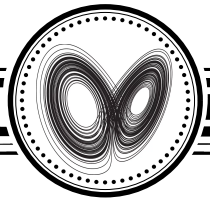

Izvestiya Vysshikh Uchebnykh Zavedeniy. Applied Nonlinear Dynamics. 2023;31(5)

Article DOI: 10.18500/0869-6632-003057

Self-oscillating systems with controlled phase of external force

D. A. Krylosova[2], *A. P. Kuznetsov*[1], *Yu. V. Sedova*[1], *N. V. Stankevich*[1,2] ✉

[1]Saratov Branch of Kotelnikov Institute of Radioengineering and Electronics of the RAS, Russia
[2]Yuri Gagarin State Technical University of Saratov, Russia
E-mail: krylosovadarina@gmail.com, kuzalexp@yandex.ru,
sedovayv@yandex.ru, ✉stankevichnv@mail.ru

Received 2.06.2023, accepted 10.08.2023, available online 12.09.2023, published 29.09.2023

Abstract. The *purpose* of this work is to study self-oscillatory systems under adaptive external action. This refers to the situation when the phase of the external action additionally depends on the dynamical variable of the oscillator. In a review plan, the results are presented for the case of a linear damped oscillator. Two cases of self-oscillatory systems are studied: the van der Pol oscillator and an autonomous quasi-periodic generator with three-dimensional phase space. *Methods.* Methods of charts of dynamical regimes and charts of Lyapunov exponents are used, as well as the construction of phase portraits and stroboscopic sections. *Results.* In a review plan, the results are presented for the case of a linear damped oscillator. Two cases of self-oscillatory systems are studied: the van der Pol oscillator and an autonomous quasi-periodic generator with a three-dimensional phase space. The pictures of characteristic dynamical regimes are described. Scenarios for the development of multidimensional chaos are described. Illustrations are given of the influence of the control parameter, which is responsible for the degree of dependence of the phase on the oscillator variable, on the dynamics of the system at different frequencies of action. *Conclusion.* The taling into account of the dependence of the phase on a dynamical variable leads to an extension of the tongues of subharmonic resonances, which are weakly expressed in the classical van der Pol oscillator. This is especially noticeable for even resonances of periods 2 and 4. For the generator of quasi-periodic oscillations in the non-autonomous case, three-frequency tori are observed, their regions begin to dominate with an increase in the adaptivity parameter, displacing the tongues of resonant two-frequency tori. A variety of multidimensional chaos characterized by an additional Lyapunov exponent close to zero is discovered, the possibility of developing hyperchaos as a result of destruction is shown.

Keywords: non-autonomous oscillator, phase, van der Pol oscillator, quasi-periodicity, chaos.

Acknowledgements. This work was supported by the Russian Science Foundation (Project no. 21-12-00121), https://rscf.ru/project/21-12-00121/

For citation: Krylosova DA, Kuznetsov AP, Sedova YuV, Stankevich NV. Self-oscillating systems with controlled phase of external force. Izvestiya VUZ. Applied Nonlinear Dynamics. 2023;31(5):549–565. DOI: 10.18500/0869-6632-003057

Introduction

In nature and technology, there are often situations when the external impact on the system depends not only on time, but also on the state of the system itself. This is a typical example of feedback. Examples in radio engineering and communication tasks can be the phase-locked frequency systems [1–5]. In biology, the system of cardiovascular regulation of living organisms increases or decreases the heart rate when the load changes [6, 7]. Similar situations are typical for neurodynamics. They can be characterized as adaptive properties of the system when the impact on it is controlled by the dynamics of the system itself.

The simplest subject for such a study can be oscillatory systems under external influence in the case when the phase of the impact depends on the dynamic variable of the system. At the same time, the autonomous system being exposed can be of different types. It is logical to choose situations that correspond to the main types of oscillatory processes. This can be the simplest damped oscillator, an auto-oscillatory system with a periodic mode, as well as a system with quasi-periodic oscillations. The first case was previously considered in detail in [8–10] and is presented as a brief overview in section 1. The following situation, which is naturally introduced into consideration — a system with periodic self-oscillations. Such a case on the example of the van der Pol system is discussed in section 2. In section 3, a controlled system with autonomous quasi-periodicity is considered — a quasi-periodic generator.

1. The case of a damped oscillator

The simplest case of an oscillatory system with a controlled phase of external action is a damped oscillator described by the equation

$$\ddot{x} + 2\alpha\dot{x} + x = A\sin(pt + kx). \tag{1}$$

Here, the initial phase of the impact depends linearly on the dynamic variable x. The system essentially depends on three parameters: the amplitude of the impact A, the frequency of the impact p, the intensity parameter of the phase control k. The normalization in the equation (1) is chosen so that the natural frequency of the oscillator is equal to one, α — the damping parameter of the oscillator.

The system (1) was discussed in detail in [8–10]. The arrangement of planes of various parameter pairs [8, 9] was investigated. It is shown that the dependence of the phase of external influence on the dynamic variable significantly complicates the dynamics. The system (1) demonstrates many areas of oscillatory modes realized in the vicinity of frequencies that are multiples of the resonant one. The possibility of bifurcations of doubling the period of oscillations and chaos is found. Multistability is also observed in the system. Other cases of dependence of the impact phase on a variable, in particular, quadratic and cubic nonlinearity [10], have also been investigated. Another control case is also discussed, when the frequency of exposure to [9] depends on the dynamic variable. A radio-electronic experimental implementation based on an oscillatory circuit with attenuation is presented for the case of both the controlled phase and the frequency of exposure [9]. We also note that in [11] a nonlinear magnetic damping oscillator with a sine-type nonlinearity and a linearly dependent phase of the effect on the angular variable is investigated.

2. The case of periodic self-oscillations — van der Pol oscillator

Let us now consider the case when the excited system can generate periodic self-oscillations. The simplest example is the van der Pol oscillator [12, 13]:

$$\ddot{x} - (\lambda - x^2)\dot{x} + x = A\sin(pt + kx). \tag{2}$$

Here λ is a control parameter responsible for negative dissipation. The other parameters are the same as in (1). The normalization is chosen so that the natural frequency of the oscillator is equal to one.

The equation (2) is reduced to the standard form of a system of three first-order equations:

$$\begin{aligned} \dot{x} &= y, \\ \dot{y} &= (\lambda - x^2)y - x + A\sin(w), \\ \dot{w} &= p + ky. \end{aligned} \tag{3}$$

Let's discuss the dynamics of the system (3). In Fig. 1, *a* presents a map of the dynamic modes of the van der Pol oscillator under harmonic influence (that is, the case of $k = 0$) on the traditional for non-autonomous systems parameter plane frequency — amplitude of the impact (p, A) for λ =1. This value of the parameter λ is convenient because it is intermediate between the cases of quasi-harmonic approximation and relaxation oscillations [12, 13]. The color on the map corresponds to the different periods of oscillation of the system, determined in the Poincare section. Since the system in question is non-autonomous, a stroboscopic section was constructed. The color palette and oscillation periods are indicated below the drawing. Non-periodic oscillations are indicated in gray (in this case they can be quasi-periodic **Q** or chaotic **C**, this method does not distinguish them). The narrow area of the run-up of trajectories is also shown **D**.

In Fig. 1, *a* one can see a vast region of period 1 corresponding to the main resonance. To the right of it are the synchronization areas on the subharmonics of the external force (in the terminology of [14]). The synchronization language corresponding to period 3 is the most pronounced, which is due to the cubic nature of the nonlinearity of the van der Pol oscillator.

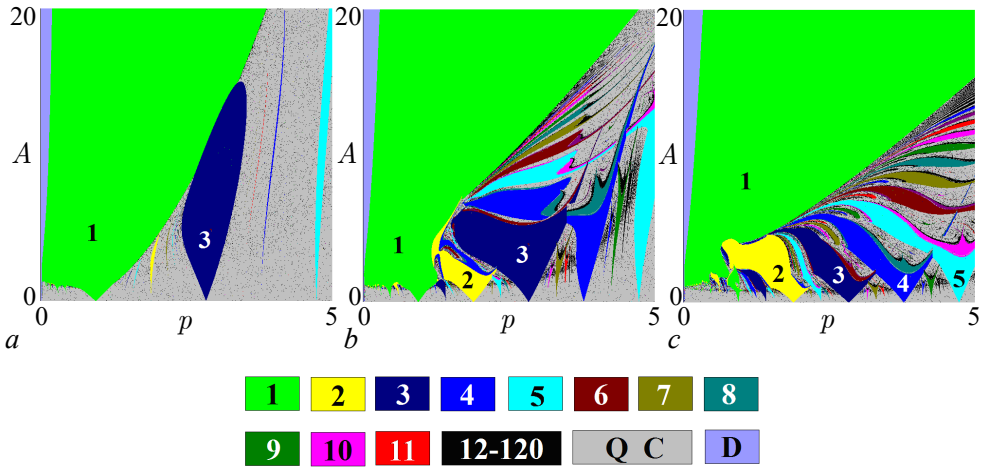

Fig 1. Charts of dynamical regimes for classical non-autonomous van der Pol oscillator (3) at $\lambda = 1$ (*a*) and with controlled phase of external force at $k = 0.5$ (*b*) and $k = 1$ (*c*) (color online)

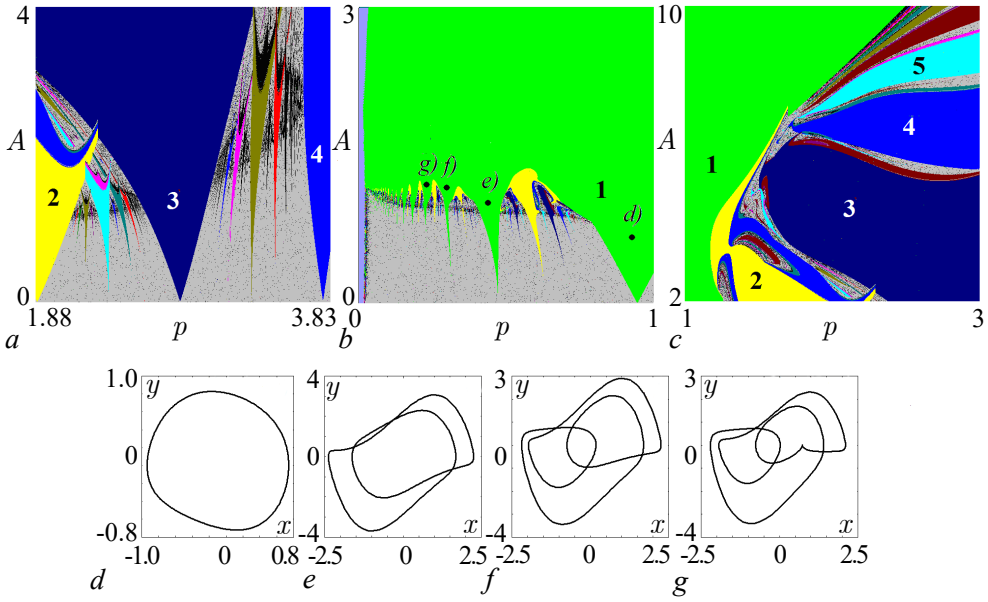

Fig 2. Zoomed fragments of chart of dynamical regime for non-autonomous van der Pol oscillator (3) at $\lambda=1$, $k=0.5$ (a, b, c). Phase portraits illustrating synchronization on the harmonics of an external force: $p = 0.92$, $A = 0.655$ (d); $p = 0.43$, $A = 1.015$ (e); $p = 0.3$, $A = 1.17$ (f); $p = 0.23$, $A = 1.2$ (g) (color online)

The effect of the phase dependence on the dynamic variable on the observed modes is illustrated in Fig. 1, b and fig. 1, c, which refer to the cases $k = 0.5$ and $k = 1$. It can be seen that the introduction of such a dependence leads to the expansion of languages in the field of synchronization on subharmonics of external force, weakly expressed in the classical van der Pol oscillator. This is especially noticeable for even resonances of periods 2 and 4. In the case of Fig. 1, c resonances with successive periods in the region of small amplitudes of the impact become "equal".

In Fig. 2 shows enlarged fragments of Fig. 1, b, illustrating the features of the device of the parameter plane. Fig. 2, a represents an enlarged area between the languages of periods 2 and 4. It can be seen that with small amplitudes of impact, the picture has become close to the classical sine mapping of the circle [15, 16]. Fig. 2, b — synchronization area on harmonics of external force (in the terminology of [14]). It is located in the frequency range less than the natural frequency of the oscillator. Such resonances on the map are characterized by a system of languages of period 1 — they are answered by a different number of revolutions of the phase trajectory, but the only intersection with the Poincare section. Examples of phase portraits for different languages of period 1 for parameter values marked with dots on the map are shown in Fig. 2, d–g. The increase in the trajectory speed is clearly visible with a decrease in the frequency of the external signal. Between the languages of period 1 in Fig. 2, b very narrow languages of other periods are also observed.

A fragment of the map in Fig. 2, c illustrates a region of sufficiently large amplitudes when, for frequencies above the proper vertex, resonant languages of different periods are pulled together to the boundary of the main resonance.

Let's discuss in more detail the influence of the control parameter k on the dynamics of the system. For this purpose, examples of maps of dynamic modes on the parameter plane (k, A) were constructed for two values of the exposure frequency: equal to the natural frequency of the oscillator $p = 1$ (Fig. 3, a) and characterized by a sufficiently large frequency by tuning $p = 5$ (fig. 3, b).

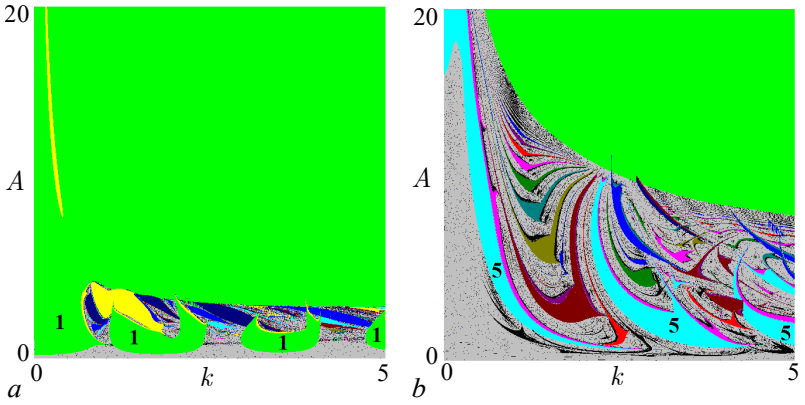

Fig 3. Charts of dynamical regime for non-autonomous van der Pol oscillator (3) at $p = 1$ (a) and $p = 5$ (b), $\lambda = 1$ (color online)

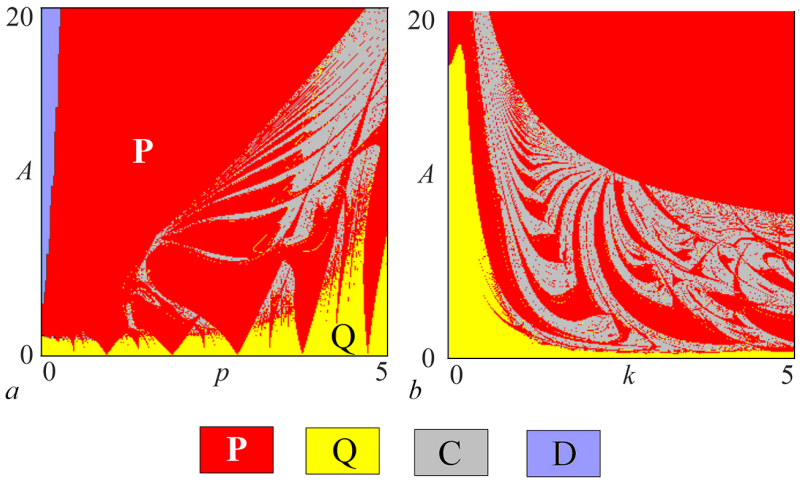

Fig 4. Charts of Lyapunov exponents for non-autonomous van der Pol oscillator (3) at $k = 0.5$ (a) and $p = 5$ (b), $\lambda = 1$ (color online)

It can be seen that when exposed at a resonant frequency of $p = 1$, with small amplitudes of exposure, a system of islands of period 1 appears, located quite regularly along the k axis. At large amplitudes of A, only the period 1 mode is observed. In turn, for the frequency of $p = 5$, a system of islands of period 5 can be seen. At the same time, with an increase in the amplitude of the impact, there are many windows of very different periods immersed in the area of irregular dynamics.

As we noted, the method used above does not distinguish between chaotic and quasi-periodic modes. In the system under consideration, however, the latter are possible (unlike in the case of a damped oscillator (1)). To demonstrate this and identify the areas of localization of these modes, examples of maps of Lyapunov exponents were constructed, shown in Fig. 4. The color on the maps was determined in accordance with the spectrum of Lyapunov exponents $\Lambda_{1,2,3}$:

P — periodic mode, $\Lambda_1 = 0$, $\Lambda_{2,3} < 0$;
Q — quasi-periodic mode, $\Lambda_{1,2} = 0$, $\Lambda_3 < 0$;
C — chaotic mode $\Lambda_1 > 0$, $\Lambda_2 = 0$, $\Lambda_3 < 0$.

A narrow area of trajectory run-up is also noted **D**.

3. The case of a three-dimensional self-oscillating system with adaptive external action — quasi-periodic generator

Now let's increase the dimension of the autonomous system to three. This creates the possibility of complicating its dynamics. Here we will consider the three-dimensional system [17, 18], which in offline mode, depending on the parameters, is able to demonstrate a state of equilibrium, periodic and quasi-periodic fluctuations. If we talk about radiophysics, then such a system can be called a quasi-periodic generator. There are several examples of such systems [17–23]. Note that quasi-periodic generators, excited even by a simple harmonic signal, have been little studied. You can specify the works of [22, 24] related to the modified by Anishchenko–Astakhov's generator, but a four-dimensional system was studied there, and within the framework of a one-parameter analysis. In the work [25], a variant of a generator without equilibrium states was studied, but in the case of pulsed action.

The system studied in this work has the form:

$$\begin{aligned} &\ddot{x} - (\lambda + z + x^2 - \beta x^4)\dot{x} + \omega_0^2 x = A\sin(pt + kx), \\ &\dot{z} = b(\varepsilon - z) - \mu\dot{x}^2. \end{aligned} \tag{4}$$

Here λ is the control parameter of the generator, and ω_0 is the frequency parameter. The other parameters are selected similarly to [17, 18]: $\varepsilon = 4$, $b = 1$, $\mu = 0.02$, $\beta = 1/18$, $\lambda = -1$. With this choice of parameters, the autonomous system (4) can exhibit both periodic and quasi-periodic fluctuations depending on the value of the parameter ω_0. We will choose two cases when $\omega_0 = 5$ and $\omega_0 = 2\pi$, which corresponds to periodic and quasi-periodic oscillations of the autonomous system. Note that the dependence of the mode type on the parameter ω_0 does not allow to exclude it by renormalization, as in the case of the van der Pol oscillator, for which the mode type does not depend on the natural frequency.

The system (4) is reduced to the standard form of four first-order equations

$$\begin{aligned} &\dot{x} = y, \\ &\dot{y} = (\lambda + z + x^2 - \beta x^4)y - \omega_0^2 x + A\sin(w), \\ &\dot{z} = b(\varepsilon - z) - \mu y, \\ &\dot{w} = p + ky. \end{aligned} \tag{5}$$

When using the Lyapunov exponent map method, it should be borne in mind that since the dimension of the autonomous system has increased, the model (5) will have 4 characteristic Lyapunov exponents $\Lambda_{1,2,3,4}$. Accordingly, there is a possibility of new dynamic modes, so we will identify:

P — periodic mode, $\Lambda_1 = 0$, $\Lambda_{2,3,4} < 0$;
Q2 — two-frequency quasi-periodic mode, $\Lambda_{1,2} = 0$, $\Lambda_{3,4} < 0$;
Q3 — three-frequency quasi-periodic mode, $\Lambda_{1,2,3} = 0$, $\Lambda_4 < 0$;
C — chaos $\Lambda_1 > 0$, $\Lambda_2 = 0$, $\Lambda_{3,4} < 0$;
C0 — chaos with an additional Lyapunov exponent close to zero $\Lambda_1 > 0$, $\Lambda_2 = 0$, $\Lambda_3 \approx 0$, $\Lambda_4 < 0$;
HC — hyperchaos $\Lambda_{1,2} > 0$, $\Lambda_3 = 0$, $\Lambda_4 < 0$.

3.1. The case of harmonic external influence on periodic and quasi-periodic oscillations. First, let's consider the case of a simple harmonic effect when $k = 0$. In Fig. 5 Lyapunov exponent maps are presented for two values of the parameter ω_0 when the autonomous

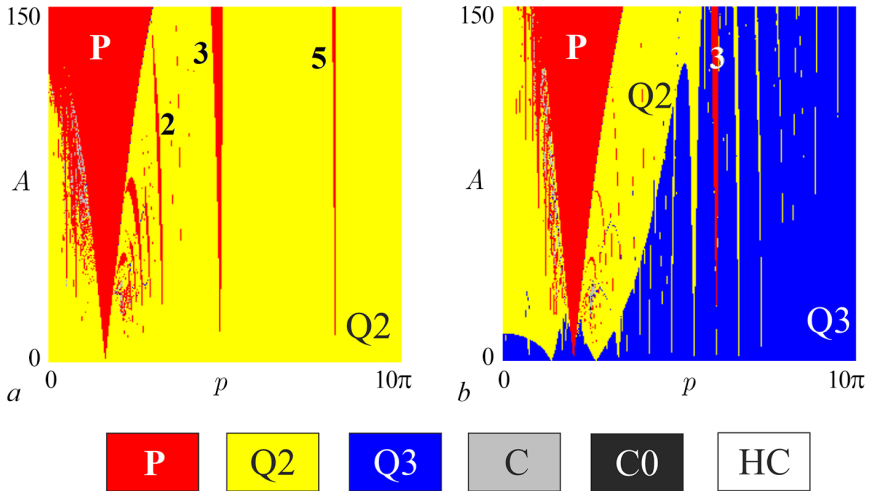

Fig 5. Charts of Lyapunov exponents of a non-autonomous quasi-periodic generator (5) for $k = 0$ and $\omega_0 = 5$ (a), $\omega_0 = 2\pi$ (b). Other parameters: $\varepsilon = 4$, $b = 1$, $\mu = 0.02$, $\beta = 1/18$, $\lambda = -1$. The numbers indicate the periods of cycles in the stroboscopic section (color online)

system demonstrates periodic and quasi-periodic self-oscillations. In the case of excitation of periodic self-oscillations (Fig. 5, a), one can see the main synchronization language **P** having a tip at a point corresponding to the frequency of external action equal to the frequency of natural oscillations of the generator. There are very narrow synchronization languages of different periods, so it is possible to distinguish resonances at double, triple and fivefold frequencies. The languages of periodic modes are immersed in the region of two-frequency quasi-periodic oscillations **Q2**. Note that near the main synchronization language, with sufficiently large signal amplitudes, a small area of chaotic behavior can be detected, which occurs when synchronization languages overlap at multiple frequencies.

In the case of a harmonic signal acting on a stable invariant torus, not only two-frequency **Q2**, but also three-frequency**Q3** quasi-periodic oscillations can be observed, Fig. 5, b. Unlike Fig. 5, a, the regions of the two-frequency tori **Q2** have the form of tongues with points located on the axis of the frequency of exposure. They are answered by resonant two-frequency tori arising on the surface of a three-frequency one. Note that an external signal can initiate periodic fluctuations of **P**, despite the fact that the autonomous system demonstrates a quasi-periodic mode. In Fig. 5, b the main synchronization language is observed, as well as a narrow language of period 3. Note that two languages of two-frequency quasi-periodicity are well traced to the right and left of the main synchronization language. Regions of chaos are possible near the main synchronization language and occupy small areas in the parameter space.

Note that the observed pattern is somewhat similar to two coupled van der Pol oscillators excited by a harmonic signal [26, 27].

3.2. The case of adaptive external influence on periodic fluctuations. Let's now consider the transformation of the pattern of modes in the system (5) in the presence of adaptability of the external signal. First, let's consider the case of $\omega_0 = 5$, when an autonomous system demonstrates periodic self-oscillations.

In Fig. 6 presents a map of dynamic modes and a Lyapunov map on the plane period — amplitude of the external signal (p, A) for the value of the adaptivity parameter $k = 5$. It is clearly seen that the presence of great adaptability leads to the destruction of the main synchronization language of period 1. However, the development of synchronization languages of other periods

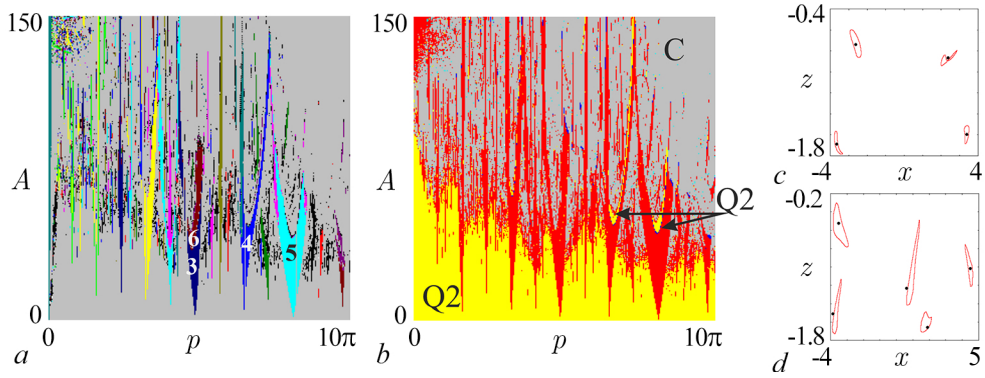

Fig 6. Chart of dynamical regime (a) and chart of Lyapunov exponents (b) for a quasi-periodic generator with an adaptive external action (5) in the regime of periodic self-oscillations, $\omega_0 = 5$, for $k = 5$. Examples of stroboscopic sections showing secondary Neimark–Sacker bifurcations inside synchronization tongues: c — $A = 45$, $p = 21$ (black), $A = 50$, $p = 21$ (red); d — $A = 46$, $p = 25$ (black), $A = 46$, $p = 25.4$ (red) (color online)

is observed — languages of period 3, 4, 5, etc. become pronounced. Inside these languages in Fig. 6, a period doubling bifurcations are well traced, for example, the region of period 6 inside the language of period 3. Within the languages of period 4 and 5, the areas of quasi-periodicity **Q2** are also visible on the map of Lyapunov exponents (marked with arrows in Fig. 6, b). They arise as a result of the Neimark–Sacker bifurcations, as illustrated by the phase portraits in stroboscopic section in Fig. 6, c and 6, d. In Fig. 6, c shows a situation when, based on the limit cycle of period 4, as a result of the Neimark–Sacker bifurcations 4-component two-frequency invariant torus is born. Fixed points in the cross section up to the bifurcation threshold are indicated in black, and invariant curves beyond the bifurcation threshold are shown in red. The parameter values are indicated in the figure caption. A similar bifurcation occurs on the basis of the synchronization language of period 5, as illustrated in Fig. 6, d.

Note that the adaptive effect leads to the formation of regions of chaos **C**, which appear as a result of overlapping synchronization languages. Significant areas of chaos are also observed at high signal amplitudes. The presence of vast regions of chaos is one of the differences from the case of the van der Pol oscillator.

3.3. The case of adaptive external influence on quasi-periodic oscillations. Now let's move on to the case when $\omega_0 = 2\pi$, and the autonomous system demonstrates two-frequency quasi-periodic oscillations. In Fig. 7 a set of maps of dynamic modes and maps of Lyapunov exponents for this situation is presented at different values of the parameter k responsible for the adaptability of the system (5).

The introduction of even low adaptability (Fig. 7, a, $k = 0.5$) changes the picture in the same way as in the case of periodic fluctuations: the main synchronization language is destroyed, while the language of period 2 becomes pronounced. On the Lyapunov exponent map it can be seen that at low amplitudes, three-frequency tori **Q3** are observed, with a built-in system of languages of two-frequency tori at combination frequencies. With increasing amplitude, the languages of the two-frequency tori overlap, forming a homogeneous region **Q2**. Very narrow languages of periodic oscillations can be found inside the languages of two-frequency tori, which expand with increasing amplitude and chaotic oscillations arise.

When the adaptivity parameter is increased to the value $k = 1$ (Fig. 7, b), the language of period 2 is also destroyed, but the languages of periods 4 and 5 become pronounced. The areas of chaos expand, while the threshold for the occurrence of chaos in amplitude A decreases.

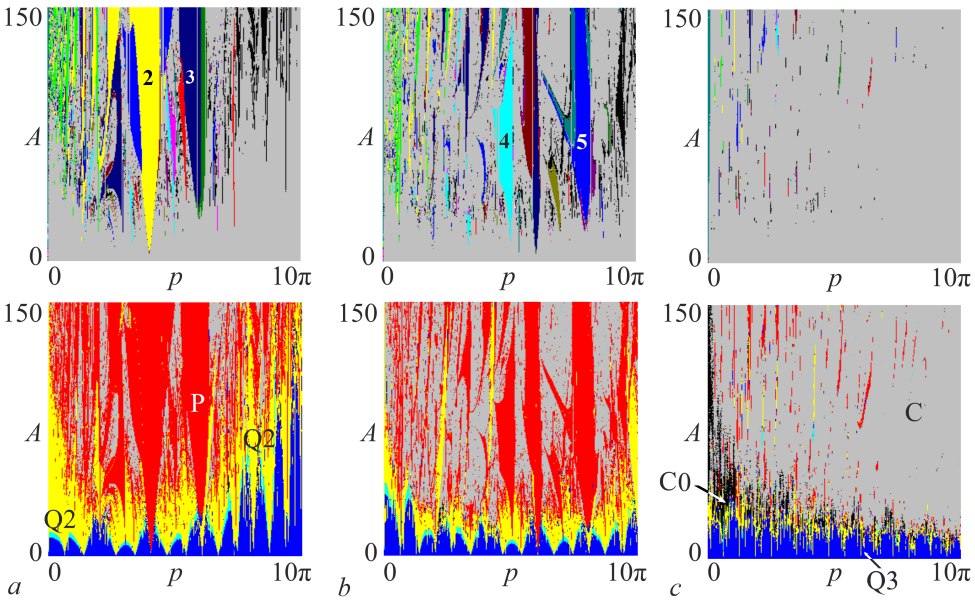

Fig 7. A set of charts of dynamic regimes (top row) and corresponding charts of Lyapunov exponents (bottom row) for a quasi-periodic generator with an adaptive external action (5) in the quasi-periodic oscillation regime, $\omega_0 = 2\pi$. $k = 0.5$ (a); $k = 1$ (b); $k = 5$ (c) (color online)

For large values of the adaptivity parameter of the external signal $k = 5$ (Fig. 7, c) on the mode map, we see that there is an almost complete disappearance of periodic modes. Only very small islands of periodicity are observed within the region of irregular oscillations. At the same time, the three-frequency tori **Q3** remain on the Lyapunov exponent map at low amplitude, which begin to dominate, displacing the languages of the two-frequency modes observed in Fig. 7, a, b.

In Fig. 8, a graphs of Lyapunov exponents in a wide range of changes in the amplitude of the external signal A for the frequency of exposure $p = 5$ and their enlarged fragments are presented, Fig. 8, b, c. With a small amplitude of the impact of A in Fig. 8, a the three-frequency quasi-periodicity of **Q3** is well traced when $\Lambda_{1,2,3} = 0$. It is illustrated by Fig. 8, d, which shows on the left the attractor of the corresponding three-frequency torus in a stroboscopic section (Fig. 8, $d1$) and on the right in a double Poincare section (Fig. 8, $d2$). When constructing a double section, the points falling into the layer $|x| < 10^{-2}$ were selected, with the additional condition $y > 0$. In the double section, one can see a smooth closed invariant curve, which corresponds to the three-frequency torus.

With an increase in the amplitude of the signal, a partial frequency capture occurs and a two-frequency torus is born. This transition occurs as a result of a saddle-node quasi-periodic bifurcation of the SNQ type described in [28], and at the moment of bifurcation a pair is born: a stable and a saddle torus. In Fig. 8, e single and double mappings for this attractor are presented. In the stroboscopic section, it is clearly visible that the invariant curve has a rather complex shape — it is multi-turn, that is, it has a large number of rotations (Fig. 8, $e1$). In the double Poincare section, 17 fixed points can be seen (Fig. 8, $e2$), which correspond to a 17-turn two-dimensional torus.

A further increase in the amplitude of the impact leads to the destruction of the two-frequency tori **Q2** and the formation of a chaotic attractor. This is illustrated by the enlarged fragment of the graphs in Fig. 8, b. Calculations show that in this case, the second indicator, as is usually accepted in numerical calculations, can be considered zero (its value is on the order of 10^{-5}). At the same time, the third Lyapunov exponent has a very small value in absolute value

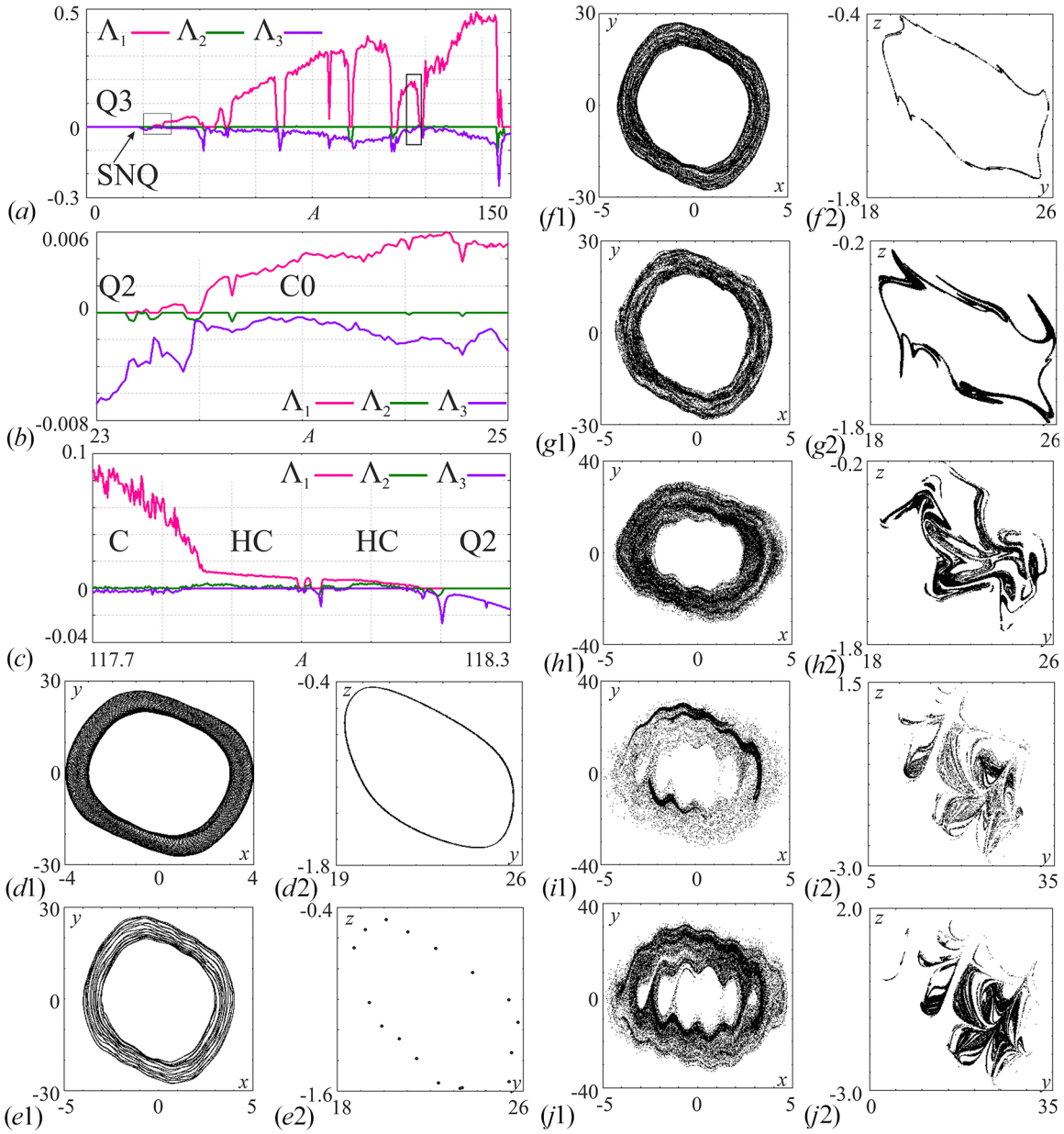

Fig 8. *a–c* — Plots of Lyapunov exponents with different scales for a quasi-periodic oscillation generator with an adaptive external action (5) in the quasi-periodic oscillation regime, $\omega_0 = 2\pi$, $k = 5$, $p = 5$. SNQ is a saddle-node bifurcation of invariant tori. Attractors of the system in the stroboscopic and double Poincaré sections: $A = 10$ (*d*); $A = 23$ (*e*); $A = 24$ (*f*); $A = 29$ (*g*); $A = 60$ (*h*); $A = 117.8$ (*i*); $A = 140.0$ (*j*) (color online)

(about 10^{-3}), but at the same time it is negative. In Fig. 8, *b* the corresponding area is indicated by **C0**. This feature of the dynamics seems interesting, and we will give some comments.

In the works [18, 29–34], the possibility of a chaotic attractor with two (or even three) zero Lyapunov exponents resulting from the destruction of a three-frequency torus or a cascade of bifurcations of doubling tori was discussed. At the same time, there are no rigorous results, and the issue is debatable. Therefore, following [18, 33], it is more accurate to talk about an additional indicator "very close to zero". In this regard, the considered example of an attractor with a third indicator close to zero but negative is interesting. This feature is most likely due to the presence of a two-dimensional saddle torus, which arose as a result of the saddle-node

bifurcation [28]. In Fig. 8, *f* presents a stroboscopic section and a double section for chaos with the third Lyapunov exponent close to zero. In the stroboscopic section, the attractor is close to a three-dimensional torus (Fig. 8, *f*1), however, in the double section we see that the invariant curve has become non-smooth and has begun to collapse, although the shape of the original invariant curve is clearly visible (Fig. 8, *f*2).

Note that on the map Fig. 7, *c* the area of dynamics of this type is shown in black and indicated by **C0**, while the value of the third indicator $\Lambda_3 \approx 0$ was determined with a threshold for fixing a value close to zero of the order of 10^{-3}. This criterion is partly conditional, since it depends on the selected threshold, but allows you to visualize the area where such dynamics are observed.

A further increase in the amplitude parameter leads to the destruction of the three-frequency torus and in Fig. 8, *g*2 in the double section we see a developed chaotic attractor, which is characterized by one positive, one zero and two negative Lyapunov exponents. An increase in the amplitude of the external signal leads to further destruction of the three-frequency torus and in Fig. 8, *h*1 already in the stroboscopic section we see that the attractor does not look like a torus; the double section demonstrates a complex chaotic attractor.

For a large amplitude of the external signal, it is also possible to detect an area where the two highest Lyapunov exponents are positive. In Fig. 8, *c* an enlarged fragment of the graphs of Lyapunov exponents is presented, where the transition to hyperhaose HC is tracked when $\Lambda_{1,2}>0$. In Fig. 8, *i* an example of a hyperchaotic attractor is presented. The interval where hyperhaos exists is quite small in the parameter space, and with a further increase in amplitude, classical chaos is realized. In Fig. 8, *j* illustrations of an attractor for large amplitudes of an external signal are presented.

Conclusion

The study of self-oscillating systems with periodic external action characterized by the property of adaptability, when the phase of the action linearly depends on the dynamic variable of the oscillator. The features of the behavior of self-oscillating autonomous systems with two-dimensional and three-dimensional phase space are considered.

The van der Pol oscillator has been studied as a two-dimensional model. The presence of adaptive effects leads to a complication of the pattern of modes, so that Arnold's languages in the field of synchronization on the subharmonics of the external signal become pronounced. Within synchronization languages, doubling bifurcations with a transition to chaos are possible. An increase in the adaptability parameter leads to the development of a pattern close to the classical sine representation of a circle.

The generator of autonomous quasi-periodicity in the mode of periodic and quasi-periodic self-oscillations is studied as a three-dimensional model. In the first case, an external influence in the presence of adaptability leads to the fact that the language of the main resonance of period 1 is destroyed, and the synchronization languages of periods 2, 3, etc. expand. Within these languages, quasi-periodic dynamics may occur due to the Neimark–Sacker bifurcations, a result, the formation of multi-turn tori occurs.

In the mode of quasi-periodic oscillations, the dynamics of a non-autonomous system becomes richer. Three-frequency quasi-periodic oscillations appear, forming a region in which the tongues of resonant two-frequency tori are immersed. In the case of a simple harmonic effect, periodic regimes of period 1, 3, etc. arise, although the autonomous system demonstrates quasi-periodicity. The presence of adaptability leads to the destruction of the main modes of

full synchronization. The domain of three-frequency quasi-periodicity is radically expanding, displacing the languages of two-frequency tori. At the same time, in small regions of the parameter space, the destruction of the three-frequency torus is observed with the formation of multi-dimensional chaos, which, in addition to zero, has another indicator close to zero in the spectrum of Lyapunov exponents. The possibility of hyperhaosis in such a system is also shown.

References

1. Best RE. Phase-Locked Loops: Design, Simulation, and Applications. 6th ed. New York: McGraw-Hill; 2007. 489 p.
2. Shalfeev VD, Matrosov VV. Nonlinear Dynamics of Phase Synchronization Systems. Nizhny Novgorod: Nizhny Novgorod University Publishing; 2013. 366 p. (in Russian).
3. Kuznetsov NV, Leonov GA. Nonlinear Mathematical Models of Phase-Locked Loops. Cambridge Scientific Publisher; 2014. 218 p.
4. Kuznetsov NV, Belyaev YV, Styazhkina AV, Tulaev AT, Yuldashev MV, Yuldashev RV. Effects of PLL architecture on MEMS gyroscope performance. Gyroscopy and Navigation. 2022;13(1):44–52. DOI: 10.1134/S2075108722010047.
5. Kuznetsov NV, Lobachev MY, Yuldashev MV, Yuldashev RV, Tavazoei MS. The gardner problem on the lock-in range of second-order type 2 phase-locked loops. IEEE Transactions on Automatic Control. 2023:1–15. DOI: 10.1109/TAC.2023.3277896.
6. Ottesen JT. Modelling the dynamical baroreflex-feedback control. Mathematical and Computer Modelling. 2000;31(4–5):167–173. DOI: 10.1016/S0895-7177(00)00035-2.
7. Hall JE. Guyton and Hall Textbook of Medical Physiology E-Book. Elsevier Health Sciences; 2015. 1147 p.
8. Seleznev EP, Stankevich NV. Complex dynamics of a non-autonomous oscillator with a controlled phase of an external force. Technical Physics Letters. 2019;45(1):57–60. DOI: 10.1134/S1063785019010334.
9. Krylosova DA, Seleznev EP, Stankevich NV. Dynamics of non-autonomous oscillator with a controlled phase and frequency of external forcing. Chaos, Solitons & Fractals. 2020;134: 109716. DOI: 10.1016/j.chaos.2020.109716.
10. Krylosova D, Seleznev E, Stankevich N. The simplest oscillators with adaptive properties. In: 2020 4th Scientific School on Dynamics of Complex Networks and their Application in Intellectual Robotics (DCNAIR). 07-09 September 2020, Innopolis, Russia. IEEE; 2020. P. 140–143. DOI: 10.1109/DCNAIR50402.2020.9216759.
11. Polczyński K, Bednarek M, Awrejcewicz J. Magnetic oscillator under excitation with controlled initial phase. In: Awrejcewicz J, Kaźmierczak M, Olejnik P, Mrozowski J, editors. 16th International Conference Dynamical Systems – Theory and Applications. 6-9 December 2021 Lódź. DSTA; 2021. P. 400–401.
12. Pikovsky A, Rosenblum M, Kurths J. Synchronization: A Universal Concept in Nonlinear Sciences. New York: Cambridge University Press; 2001. 412 p. DOI: 10.1017/CBO97805 11755743.
13. Balanov A, Janson N, Postnov D, Sosnovtseva O. Synchronization: From Simple to Complex. Berlin: Springer; 2009. 426 p. DOI: 10.1007/978-3-540-72128-4.
14. Landa PS. Self-Oscillations in Systems With a Finite Number of Degrees of Freedom. Moscow: Nauka; 1980. 360 p. (in Russian).
15. Ding EJ, Hemmer PC. Winding numbers for the supercritical sine circle map. Physica D: Nonlinear Phenomena. 1988;32(1):153–160. DOI: 10.1016/0167-2789(88)90092-9.

16. Ivankov NY, Kuznetsov SP. Complex periodic orbits, renormalization, and scaling for quasiperiodic golden-mean transition to chaos. Phys. Rev. E. 2001;63(4):046210. DOI: 10.1103/PhysRevE.63.046210.
17. Kuznetsov AP, Kuznetsov SP, Mosekilde E, Stankevich NV. Generators of quasiperiodic oscillations with three-dimensional phase space. The European Physical Journal Special Topics. 2013;222(10):2391–2398. DOI: 10.1140/epjst/e2013-02023-x.
18. Kuznetsov AP, Kuznetsov SP, Shchegoleva NA, Stankevich NV. Dynamics of coupled generators of quasiperiodic oscillations: Different types of synchronization and other phenomena. Physica D: Nonlinear Phenomena. 2019;398:1–12. DOI: 10.1016/j.physd.2019.05.014.
19. Matsumoto T. Chaos in electronic circuits. Proceedings of the IEEE. 1987;75(8):1033–1057. DOI: 10.1109/PROC.1987.13848.
20. Anishchenko VS, Nikolaev SM. Generator of quasi-periodic oscillations featuring two-dimensional torus doubling bifurcations. Technical Physics Letters. 2005;31(10):853–855. DOI: 10.1134/1.2121837.
21. Anishchenko V, Nikolaev S, Kurths J. Winding number locking on a two-dimensional torus: Synchronization of quasiperiodic motions. Phys. Rev. E. 2006;73(5):056202. DOI: 10.1103/PhysRevE.73.056202.
22. Anishchenko V, Nikolaev S, Kurths J. Peculiarities of synchronization of a resonant limit cycle on a two-dimensional torus. Phys. Rev. E. 2007;76(4):046216. DOI: 10.1103/PhysRevE.76.046216.
23. Kuznetsov AP, Kuznetsov SP, Stankevich NV. A simple autonomous quasiperiodic self-oscillator. Communications in Nonlinear Science and Numerical Simulation. 2010;15(6):1676–1681. DOI: 10.1016/j.cnsns.2009.06.027.
24. Kuznetsov AP, Sedova YV. Anishchenko-Astakhov quasiperiodic generator excited by external harmonic force. Technical Physics Letters. 2022;48(2):84–86. DOI: 10.21883/TPL.2022.02.52858.18925.
25. Stankevich NV, Kuznetsov AP, Kurths J. Forced synchronization of quasiperiodic oscillations. Communications in Nonlinear Science and Numerical Simulation. 2015;20(1):316–323. DOI: 10.1016/j.cnsns.2014.04.020.
26. Kuznetsov AP, Sataev IR, Turukina LV. Phase dynamics of periodically driven quasiperiodic self-vibrating oscillators. Izvestiya VUZ. Applied Nonlinear Dynamics. 2010;18(4):17–32 (in Russian). DOI: 10.18500/0869-6632-2010-18-4-17-32.
27. Kuznetsov AP, Sataev IR, Turukina LV. Forced synchronization of two coupled van der Pol self-oscillators. Russian Journal of Nonlinear Dynamics. 2011;7(3):411–425 (in Russian). DOI: 10.20537/nd1103001.
28. Vitolo R, Broer H, Simó C. Quasi-periodic bifurcations of invariant circles in low-dimensional dissipative dynamical systems. Regular and Chaotic Dynamics. 2011;16(1–2):154–184. DOI: 10.1134/S1560354711010060.
29. Broer H, Simó C, Vitolo R. Bifurcations and strange attractors in the Lorenz-84 climate model with seasonal forcing. Nonlinearity. 2002;15(4):1205–1267. DOI: 10.1088/0951-7715/15/4/312.
30. Broer HW, Simó C, Vitolo R. Chaos and quasi-periodicity in diffeomorphisms of the solid torus. Discrete and Continuous Dynamical Systems - B. 2010;14(3):871–905. DOI: 10.3934/dcdsb.2010.14.871.
31. Stankevich NV, Shchegoleva NA, Sataev IR, Kuznetsov AP. Three-dimensional torus breakdown and chaos with two zero Lyapunov exponents in coupled radio-physical generators.

Journal of Computational and Nonlinear Dynamics. 2020;15(11):111001. DOI: 10.1115/1.4048025.
32. Grines EA, Kazakov A, Sataev IR. On the origin of chaotic attractors with two zero Lyapunov exponents in a system of five biharmonically coupled phase oscillators. Chaos: An Interdisciplinary Journal of Nonlinear Science. 2022;32(9):093105. DOI: 10.1063/5.0098163.
33. Karatetskaia E, Shykhmamedov A, Kazakov A. Shilnikov attractors in three-dimensional orientation-reversing maps. Chaos: An Interdisciplinary Journal of Nonlinear Science. 2021; 31(1):011102. DOI: 10.1063/5.0036405.
34. Kuznetsov AP, Sedova YV, Stankevich NV. Coupled systems with quasi-periodic and chaotic dynamics. Chaos, Solitons & Fractals. 2023;169:113278. DOI: 10.1016/j.chaos.2023.113278.